First principles study of the magnetism driven by cation defects in CeO_2: the important role of O2p states*

Lu Zhan-Sheng(路战胜)[a], Ma Dong-Wei(马东伟)[a], Zhang Jing(张 静)[b], Xu Guo-Liang(徐国亮)[a], and Yang Zong-Xian(杨宗献)[a]†

[a] *College of Physics and Information Engineering and Henan Key Laboratory of Photovoltaic Materials, Henan Normal University, Xinxiang* 453007, *China*

[b] *School of Mathematics and Information Science, North China University of Water Resources and Electric Power, Zhengzhou* 450011, *China*

(Received 13 September 2011; revised manuscript received 3 November 2011)

The magnetism driven by cation defects in undoped CeO_2 bulk and thin films is studied by the density functional theory corrected for on-site Coulomb interactions (DFT+U) with $U = 5$ eV for the Ce4f states and $U = 7$ eV for the O2p states. It is found that the Ce vacancies can induce a magnetic moment of the ~ 4 μ_B/supercell, which arises mainly from the 2p hole state of the nearest neighbouring O atom (~ 1 μ_B on per oxygen) to the Ce vacancy. The effect of the methodology is investigated, indicating that $U = 7$ eV for the O2p state is necessary to obtain the localized O2p hole state in defective ceria with cation vacancies.

Keywords: magnetism, cation defect, CeO2, density functional theory

PACS: 75.70.–I, 71.15.Mb, 75.47.Pq, 71.15.–m **DOI:** 10.1088/1674-1056/21/4/047505

1. Introduction

Much effort has been made to investigate dilute magnetic semiconductors (DMSs) due to their peculiar magnetic properties for potential spintronic applications. Metal oxides have been an intense research subject for applications in the spintronic field[1] since the discovery of room-temperature ferromagnetism (FM) in DMS oxide systems.[2–4] FM has been found in HfO_2 thin films on sapphire or silicon substrates without any doping,[5,6] so-called "d^0 ferromagnetism".[7] FM behaviour has also been experimentally found in other undoped non-magnetic metal oxides, such as thin films of TiO_2 and In_2O_3,[8] and in nanoparticles of CeO_2, SnO_2, and ZnO.[9,10] Moreover, diluted defect magnetism was suggested as a universal feature of ferromagnetism in nonmagnetic oxides without magnetic impurities.[10]

As a wide band gap insulator, ceria has been studied as a possible DMS material. However, the explanation for FM behaviour in CeO_2 nanoparticles has been a source of controversy.[11] Recent theoretical and experimental results[11–13] have suggested that the ferromagnetic behaviour in pure CeO_2 at ambient temperature can be induced by oxygen vacancies (anion vacancies), which cause spin polarization of the Ce4f states surrounding the oxygen vacancies. On the other hand, Liu *et al.*[14] concluded that it was Ce vacancies, not oxygen vacancies, as a potential FM causing defect could be responsible for FM behaviour in the CeO_2 nanoparticles, and it is found that the neutral cation vacancies in CaO,[15] HfO_2,[16] TiO_2,[17] ZnO,[18,19] MgO,[20] SnO_2,[21] CeO_2,[10] and so on, can induce local magnetic moments on its neighbouring atoms and that the moments order ferromagnetically.

2. Computational methods

In the present study, we carry out first principles calculations of the cation vacancy effect on the ferromagnetism of CeO_2 bulk and thin films. Our research shows that like other ionic materials, the cation vacancies in CeO_2 do induce ferromagnetism. All of the calculations are performed using the Vienna *ab initio* Simulation Package (VASP)[22–25] based on density functional theory (DFT). The electron–ion interaction is described by the PAW (projector-augmented

*Project supported by the National Natural Science Foundation of China (Grant Nos. 11174070, 10947001, and 11004066), the Innovation Scientists and Technicians Troop Construction Projects of Henan Province, China (Grant No. 104200510014), and the Foundation for University Young Core Instructors of Henan Province, China (Grant No. 2009GGJS-044).

†Corresponding author. E-mail: yzx@henannu.edu.cn

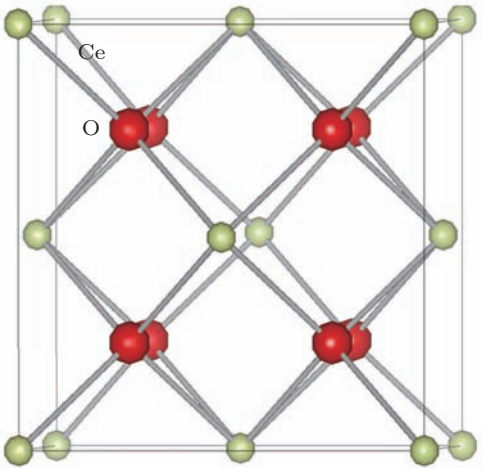
© 2012 Chinese Physical Society and IOP Publishing Ltd

wave) method,[26,27] and the PBE (Perdew–Burke–Ernzerhof) functional[28] is employed to deal with the electron–electron exchange–correlation energies. Twelve electrons from the $5s^2 5p^6 6s^2 4f^1 5d^1$ of Ce and six electrons from the $2s^2 2p^4$ of the O are treated as valance electrons.

The description of the electronic structure of reduced CeO_2 from the regular DFT-GGA has been shown to be inconsistent with experimental results, in that no gap state between the valence band and the unoccupied Ce4f states is present.[29] Thus, the DFT+4U method has been applied to partially reduced ceria systems.[30,31] The superiority of DFT+U to DFT has also been shown for the description of reduced ceria.[30,31] In a DFT+U calculation, the U parameter for the Ce4f state is determined empirically and there are several studies[30−32] in which how the value of U is fitted against the experimental results is described. According to the recent tests,[30−32] the DFT+U method ($U^{\mathrm{Ce4f}} = 5$ eV) is used to correct the strong on-site Coulomb repulsion of Ce4f states. More details of this approach and the choice of U^{Ce4f} have been discussed extensively in earlier studies.[30−32]

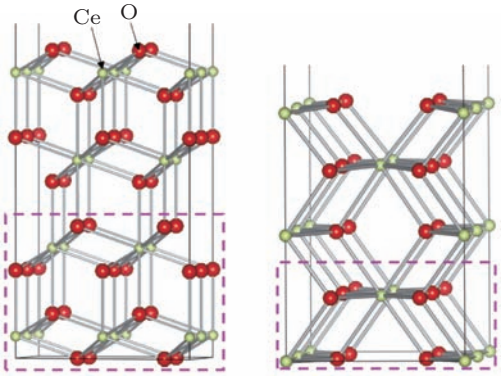
It is well known that creating a cation vacancy or substituting an M^{n+} cation with a lower valence $M^{(n-1)+}$ cation in a metal oxide leads to the formation of a localized electronic hole on an oxygen atom neighbouring the dopant. This electronic hole gives rise to issues with the description of the resulting electronic structure using DFT, due to being without the U term on the O2p states, and it is found that the hole is delocalized over several oxygen atoms. The details have been discussed in Li-doped MgO and Si-doped Al_2O_3.[33,34] Upon formation of the Ce vacancies, the O2p holes will be present, and this kind of cationic defect can be well described with DFT+U ($U^{\mathrm{O2p}} = 7$ eV)—as demonstrated by Nolan and Watson for the Li-doped MgO,[33] Al-doped SiO_2[34] and by Yeriskin and Nolan[35,36] for La-doped CeO_2. In line with Yeriskin and Nolan's studies,[35,36] the DFT+U with $U^{\mathrm{O2p}} = 7$ eV is used to describe the O2p states. Hereafter, the DFT+U with only $U^{\mathrm{Ce4f}} = 5$ eV method will be denoted as the "DFT+U^{Ce4f} method" and the DFT+U method with both $U^{\mathrm{Ce4f}} = 5$ eV and $U^{\mathrm{O2p}} = 7$ eV will be referred to as the "DFT+$U^{\mathrm{Ce4f\ and\ O2p}}$ method".

Bulk crystalline CeO_2 has a fluorite structure and one Ce atom is surrounded by eight oxygen atoms (Fig. 1). The calculated lattice parameter of the CeO_2 is 5.42 Å (1 Å=0.1 nm) from the DFT+$U^{\mathrm{Ce4f\ and\ O2p}}$ method. The 96-site cell, built from the conventional 12-atom cubic unit cell of CeO_2 (Fig. 1) with a 2×2×2 replication, was modeled to calculate the ceria bulk. Similar to the recent studies on the O vacancy formation in CeO_2,[37] balancing both the computational efficiency and accuracy, only one k point (the gamma point) was used for all the calculations on the 96-site cell.[38] The ceria thin films, i.e. the CeO_2 (111) and (110) surfaces, were modeled using the slab models in a three-dimensional (3D) periodic construction (Fig. 2). Four O–Ce–O triple-layers with a $P(2\times2)$ surface supercell for CeO_2 (111) and five CeO_2 layers with a $P(2\times1)$ surface supercell for CeO_2 (110), each with a vacuum gap of 15 Å were included in the computational boxes, respectively. The two lowest layers (see Fig. 2) were kept fixed at the optimized bulk values, while all other atoms were allowed to relax. The Brillouin-zone integrations were performed with a 4×4×1 Monkhorst–Pack grid.[38] For all of the calculations, plane-waves



CeO_2 bulk

Fig. 1. (colour online) A conventional 12-atom cubic unit cell of CeO_2.



(a) (b)

Fig. 2. (colour online) Slab models for ceria surfaces: (a) CeO_2 (111) $p(2\times2)$; (b) CeO_2 (110) $p(1\times2)$. The bottom six [for the (111) surface] or two [for the (110) surface] atomic layers are fixed at their bulk positions. The slabs are repeated in the z direction, and between the slabs there is a 15 Å-thick vacuum layer.

have been included up to an energetic cutoff of 30 Ry (1 Ry=13.605 eV). The structure optimizations were performed until the force on each atom was less than 0.02 eV/Å. Charge analysis was performed according to the Bader-type charge analysis method.[39]

Stoichiometric CeO_2 is non-magnetic. Upon an oxygen atom moving away from its lattice position, the two electrons are left behind and localized on the 4f states of two of the neighbouring cerium atoms, turning Ce^{4+} into Ce^{3+}.[40] The induced ferromagnetism from the oxygen vacancy in ceria has been studied clearly.[11−13] Moreover, the effect of the Ce vacancy in ceria has been studied by Fernandes *et al.*[10] using the smaller size bulk cells, i.e. 12-sites, 24-sites, and 48-sites, respectively, within the DFT+U^{Ce4f} method. Thus the exact destinations of the oxygen holes and the localized O2p electrons were not found as shown in the following. Here, the ferromagnetism driven by cation defects in a larger 96-site CeO_2 bulk cell and ceria thin films will be focused within the DFT+$U^{\mathrm{Ce4f\ and\ O2p}}$ method.

3. Results and discussion

According to the theoretical research of CaO, TiO_2, and HfO_2, in the perfect crystal, the O2p states are fully filled and form the valence band. Since Ce is a cation with a 4+ valence, the removal of one neutral Ce atom introduces four empty states (holes) among the O2p states. The spin occupation of these four states determines whether the system is magnetic.

To investigate the destinations of the oxygen holes, the spin density (the difference in electron density between spin-up and spin-down channels) and the O2p partial electronic density of states (PEDOS) of the nearest neighbouring (NN) O atoms to the Ce vacancy are presented in Figs. 3(a) and 3(b), respectively. It is found that the spin density is strongly localized on the four nearest neighbouring oxygen atoms to the Ce vacancy (Fig. 3(a)), with a spin moment of 0.95 μ_B per oxygen. The spin moments on the remaining O and Ce atoms are negligible, resulting in a total moment of 4.00 μ_B in the supercell, which corresponds to the number of holes. The predominant localization of the holes on the oxygen atoms near the Ce vacancy is similar to the behaviour for other similar systems.[35,36]

By comparison with the La-doped ceria (111) surface with DFT+$U^{\mathrm{Ce4f\ and\ O2p}}$ method,[35] a similar profile of the O2p PEDOS was found in our ceria systems with Ce vacancy (Fig. 3(b)), which shows several significant peaks (e.g., two of the peaks are located in the valence band region at −5.2 eV and −4.0 eV, respectively, below the Fermi energy, and the third is at 1.5 eV above the Fermi energy). The formation of the localized O^- species is identified by the significant peaks above the Fermi energy in the PEDOS, which is different from that of a delocalized O^- species (which will be discussed in the following). Thus, the strong localized O2p states in the CeO_2 with the cation defect are found from the DFT+$U^{\mathrm{Ce4f\ and\ O2p}}$ method.

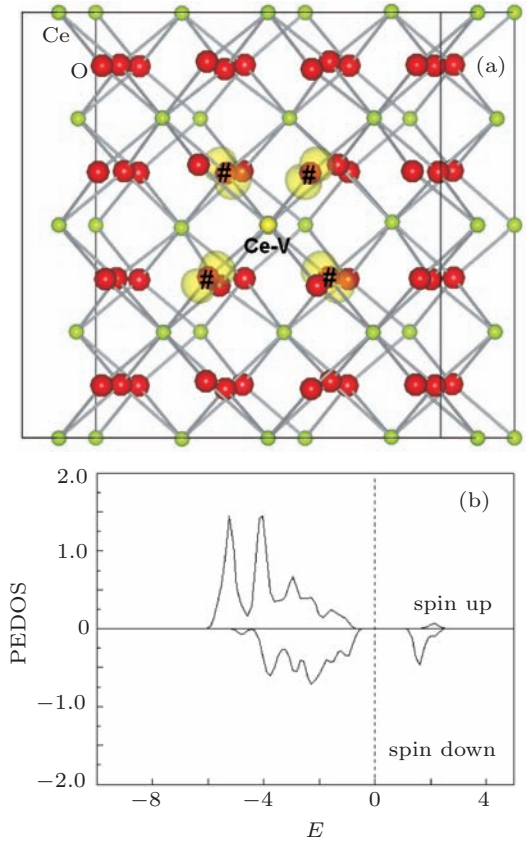


Fig. 3. (colour online) The properties of CeO_2 bulk with Ce vacancy from the DFT+$U^{\mathrm{Ce4f\ and\ O2p}}$ method: (a) the spin density, and the isosurface value used is ± 0.02 e/Å^3 (hereafter, the Ce vacancy is denoted as "Ce-V"); (b) the partial electronic density of states (PEDOS) of the O2p states for the hole-carrying oxygen denoted as "#" in panel (a).

To investigate the effects of surface defects on the magnetism of the CeO_2 thin film, calculations were also carried out on CeO_2 (111) and (110) surfaces as modeled above. The Ce vacancy was generated by removing a Ce atom separately from the (111) and (110) surfaces. Similar to the O vacancies,[11] the presence of Ce vacancies leads to the formation of local moments in the surfaces. Basically, one Ce vacancy acting as an acceptor can leave four holes as mentioned above and the calculated total magnetic moment is 4.00 μ_B

from the DFT+$U^{\text{Ce4f and O2p}}$ method. To further visualize the change in magnetic property resulting from Ce vacancies, the spin densities and the PEDOS for the polarized O atoms are shown in Figs. 4 and 5, respectively. Similar to the results of the ceria bulk with Ce vacancy as given above, the main contribution to the total magnetic moment arises from the 2p states of the four O atoms neighbouring the vacancy, and each of them has a magnetic moment of $\sim 1.0\ \mu_B$, while the magnetic moments on Ce and other O atoms are almost negligible. The significant peaks above the Fermi energy in PEDOS (Fig. 5) confirm the formation of the localized O^- species in the ceria (111) and (110) surface with Ce vacancies.

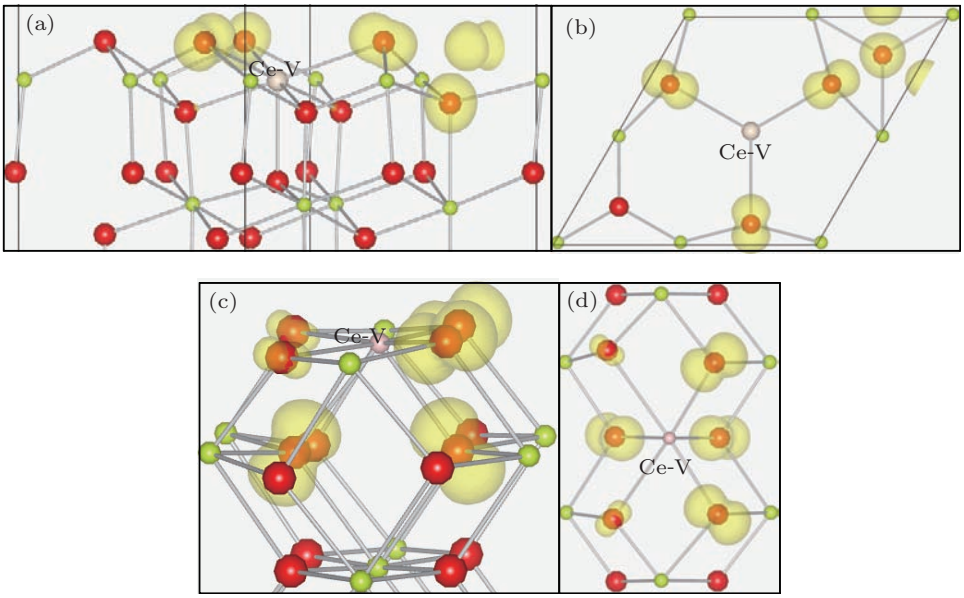


Fig. 4. (colour online) Spin densities of the CeO_2 (111) and (110) surfaces with Ce vacancies: panels (a) and (b) show the side view and top view of the CeO_2 (111) surface, respectively; and panels (c) and (d) display the side and top views of the CeO_2 (110) surface.

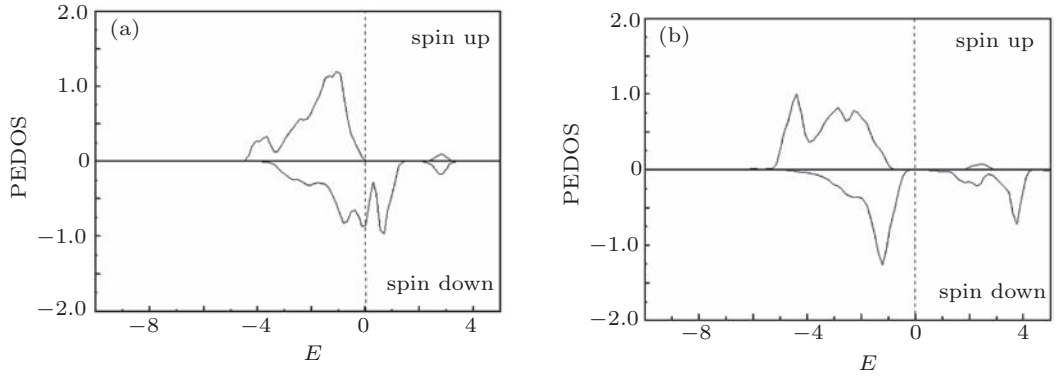


Fig. 5. (colour online) The PEDOS of the O2p states for the hole-carrying oxygen: (a) in the CeO_2 (111) surface with Ce vacancy; (b) in the CeO_2 (110) surface with Ce vacancy.

As mentioned above, due to the strong on-site Coulomb repulsion, the DFT+U^{Ce4f} method has been used to calculate the properties of the CeO_2 with O vacancies.[30−32] The dependence of the energetic and electronic properties for the CeO_2 with O vacancies on the U value has been studied in Refs. [30]–[32]. On the other hand, the DFT+U with $U^{\text{O2p}} = 7$ eV method has been used to describe the hole states introduced by the La dopant in ceria surfaces.[35,36] However, the effect of the methodology on the properties of the CeO_2 with Ce vacancies is still lacking. To this end, the effect of the different methods, i.e. the DFT+U^{Ce4f} method and the DFT+$U^{\text{Ce4f and O2p}}$ method, on the properties (especially the magnetic properties) of the CeO_2 with Ce vacancies will be focused on in the following.

The CeO_2 bulk with Ce vacancy is studied from both the DFT+U^{Ce4f} method and the DFT+$U^{Ce4f\ and\ O2p}$ method. Without U^{O2p} on oxygen, the holes introduced by the Ce vacancy in the CeO_2 bulk are delocalized mainly over the eight NN oxygen atoms to the Ce vacancy with a computed spin moment of $\sim 0.25\ \mu_B$ per oxygen (Fig. 6(a)). The spin moments on the next NN oxygen atoms to the Ce vacancy are one order of magnitude smaller ($\sim 0.05\ \mu_B$), and those on the remaining O atoms and Ce atoms are negligible, resulting in a total spin moment of 4.00 μ_B in the supercell. As shown above, with U^{O2p}, the spin density is strongly localized on the four NN oxygen atoms to the Ce vacancy (Fig. 3(a)), with a computed spin moment of 0.95 μ_B per oxygen.

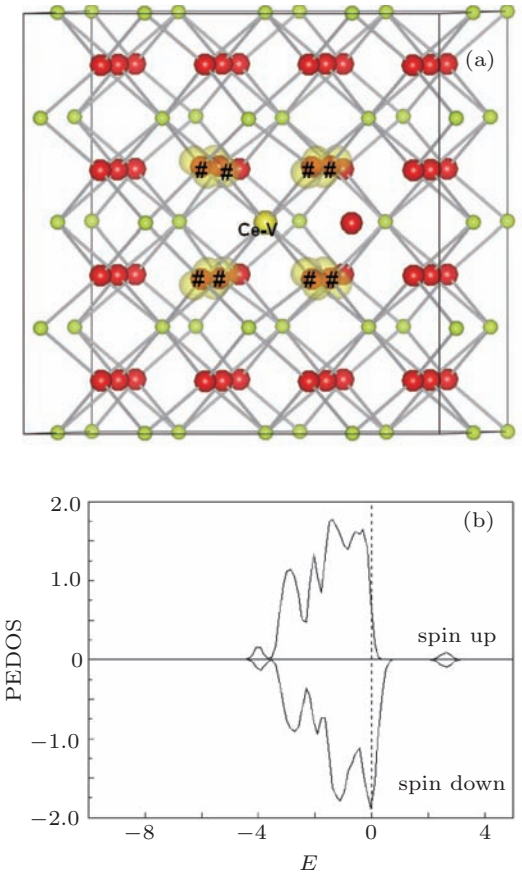


Fig. 6. (colour online) The properties of CeO_2 bulk with Ce vacancy from the DFT+U^{Ce4f} method: (a) the spin density; and (b) the PEDOS of the O2p states for the oxygen atom denoted as "#" in panel (a).

On the other hand, it is found that there is an immediate difference between the two descriptions in comparison with the PEDOS (Fig. 3(b) and Fig. 6(b)) with and without using U^{O2p} on oxygen, i.e. the DFT+$U^{Ce4f\ and\ O2p}$ method and DFT+U^{Ce4f} method. From the DFT+U^{Ce4f} method, the plotted profile of the PEDOS for the O atom is quite similar to that for the TiO_2 with Ti vacancy[17] and SnO_2 with Sn vacancy[21] systems, and the spin-polarization of the O2p states located at the Fermi energy is the major reason for the magnetism. Thus, the profile corresponds to $\sim 0.25\ \mu_B$ per oxygen, which is a delocalized O^- species[35] and shows a very different PEDOS structure from that of the localized O^- species shown in Fig. 3(b).

According to the above comparison, for the CeO_2 with cation vacancies, a very different localization of the O2p hole states can be reached with the DFT+U^{Ce4f} method and the DFT+$U^{Ce4f\ and\ O2p}$ method. The DFT+U^{Ce4f} method results in delocalized O2p hole states, while the DFT+$U^{Ce4f\ and\ O2p}$ method gives strong localized O2p hole states. These should be the original reasons for finding the delocalized or partially localized O2p states in the other research on metal oxides with cation vacancies, such as TiO_2,[17] SnO_2,[21] CeO_2,[10] and HfO_2.[16]

4. Conclusion

The electronic and magnetic properties of CeO_2 bulk and thin films are studied using density functional theory calculations. The results show that spin polarization can be introduced by the cation vacancy, i.e. Ce vacancy. Each Ce vacancy results in a total spin moment of 4.00 μ_B, which corresponds to the number of holes induced due to the creation of the Ce vacancy. The local magnetic moments arise mainly from the O2p hole states of the O atoms neighbouring the Ce vacancy, which holds a spin moment of $\sim 1\ \mu_B$ per oxygen from the DFT+$U^{Ce4f\ and\ O2p}$ method. The DFT+$U^{Ce4f\ and\ O2p}$ method gives a strong localization of the O2p hole states for the CeO_2 with the cation vacancy, and therefore can well describe the cation-defect systems. In contrast, the DFT+U^{Ce4f} method gives a delocalized O2p hole state. Thus, the predictive capability of the DFT+$U^{Ce4f\ and\ O2p}$ method will be useful for studying O2p hole states in doped and defective oxide materials.[34]

Acknowledgement

The calculations were performed at the high-performance computing center of the College of Physics and Information Engineering, Henan Normal University.

References

[1] Žutić I, Fabian J and Das Sarma S 2004 *Rev. Mod. Phys.* **76** 323

[2] Coey J M D, Venkatesan M and Fitzgerald C B 2005 *Nat. Mater.* **4** 173

[3] MacDonald A H, Schiffer P and Samarth N 2005 *Nat. Mater.* **4** 195

[4] Jungwirth T, Sinova J, Mašek J, Kučera J and MacDonald A H 2006 *Rev. Mod. Phys.* **78** 809

[5] Venkatesan M, Fitzgerald C B and Coey J M D 2004 *Nature* **430** 630

[6] Coey J M D, Venkatesan M, Stamenov P, Fitzgerald C B and Dorneles L S 2005 *Phys. Rev.* B **72** 024450

[7] Coey J M D 2005 *Solid State Sci.* **7** 660

[8] Hong N H, Sakai J, Poirot N and Briz V 2006 *Phys. Rev.* B **73** 132404

[9] Sundaresan A, Bhargavi R, Rangarajan N, Siddesh U and Rao C N R 2006 *Phys. Rev.* B **74** 161306

[10] Fernandes V, Mossanek R J O, Schio P, Klein J J, de Oliveira A J A, Ortiz W A, Mattoso N, Varalda J, Schreiner W H, Abbate M and Mosca D H 2009 *Phys. Rev.* B **80** 035202

[11] Keating P R L, Scanlon D O and Watson G W 2009 *J. Phys.: Condens. Matter* **21** 405502

[12] Han X, Lee J and Yoo H I 2009 *Phys. Rev.* B **79** 100403

[13] Ge M Y, Wang H, Liu E Z, Liu J F, Jiang J Z, Li Y K, Xu Z A and Li H Y 2008 *Appl. Phys. Lett.* **93** 062505

[14] Liu Y, Lockman Z, Aziz A and MacManus-Driscoll J 2008 *J. Phys.: Condens. Matter* **20** 165201

[15] Elfimov I S, Yunoki S and Sawatzky G A 2002 *Phys. Rev. Lett.* **89** 216403

[16] Das Pemmaraju C and Sanvito S 2005 *Phys. Rev. Lett.* **94** 217205

[17] Yu B and Qiang C 2008 *Phys. Status Solidi (RRL)* **2** 25

[18] Wang Q, Sun Q, Chen G, Kawazoe Y and Jena P 2008 *Phys. Rev.* B **77** 205411

[19] Xiao Z L and Shi L B 2011 *Acta Phys. Sin.* **60** 027502 (in Chinese)

[20] Wang F, Pang Z, Lin L, Fang S, Dai Y and Han S 2009 *Phys. Rev.* B **80** 144424

[21] Zhang C W, Kao H and Dong J M 2009 *Phys. Lett.* A **373** 2592

[22] Kresse G and Furthmuller J 1996 *Comput. Mater. Sci.* **6** 15

[23] Kresse G and Hafner J 1993 *Phys. Rev.* B **47** 558

[24] Kresse G and Hafner J 1994 *Phys. Rev.* B **49** 14251

[25] Kresse G and Furthmüller J 1996 *Phys. Rev.* B **54** 11169

[26] Kresse G and Joubert D 1999 *Phys. Rev.* B **59** 1758

[27] Blöchl P E 1994 *Phys. Rev.* B **50** 17953

[28] Perdew J P, Burke K and Ernzerhof M 1996 *Phys. Rev. Lett.* **77** 3865

[29] Yang Z, Woo T K, Baudin M and Hermansson K 2004 *J. Chem. Phys.* **120** 7741

[30] Nolan M, Grigoleit S, Sayle D C, Parker S C and Watson G W 2005 *Surf. Sci.* **576** 217

[31] Nolan M, Parker S C and Watson G W 2005 *Surf. Sci.* **595** 223

[32] Castleton C W M, Kullgren J and Hermansson K 2007 *J. Chem. Phys.* **127** 244704

[33] Nolan M and Watson G W 2005 *Surf. Sci.* **586** 25

[34] Nolan M and Watson G W 2006 *J. Chem. Phys.* **125** 144701

[35] Yeriskin I and Nolan M 2010 *J. Phys.: Condens. Matter* **22** 135004

[36] Yeriskin I and Nolan M 2009 *J. Chem. Phys.* **131** 244702

[37] Jiang Y, Adams J B, Schilfgaarde M V, Sharma R and Crozier P A 2005 *Appl. Phys. Lett.* **87** 141917

[38] Monkhorst H J and Pack J D 1976 *Phys. Rev.* B **13** 5188

[39] Henkelman G, Arnaldsson A and Jónsson H 2006 *Comput. Mater. Sci.* **36** 354

[40] Skorodumova N V, Simak S I, Lundqvist B I, Abrikosov I A and Johansson B 2002 *Phys. Rev. Lett.* **89** 166601